**ELECTRONIC SUPPLEMENTARY MATERIALS**
***Proceedings of the Royal Society Biology***

# Olfaction written in bone: Cribriform plate size parallels olfactory receptor gene repertoires in Mammalia

Deborah J. Bird[1, 4,]*, William J. Murphy[2], Lester Fox-Rosales[1], Iman Hamid[1], Robert A. Eagle[3], Blaire Van Valkenburgh[1]

[1]Department of Ecology and Evolutionary Biology, University of California Los Angeles, 610 Charles E. Young Dr. S., Los Angeles, CA 90095-8347, USA.
[2]Department of Veterinary Integrative Biosciences, Texas A&M University, College Station, Texas 77843-4458, USA
[3]Department of Atmospheric and Oceanic Sciences, Institute of the Environment and Sustainability, University of California Los Angeles, 520 Portola Plaza, Math Sciences Building 7127, Los Angeles, CA 90095, USA.
[4]Lead Contact
*Correspondence: dbirdseed@gmail.com

**Supplementary movie S1. Movie of cribriform plate and nasal anatomy within skull.** Animated 3D model of an Arctic fox (*Vulpes lagopus*) skull featuring the cribriform plate and general nasal anatomy. The cribriform plate (red) model clearly displays the perforations, or foramina, through which axon bundles from olfactory sensory neurons pass en route to the olfactory bulb of the brain. Sensory neurons in the olfactory epithelium are located primarily on the ethmoturbinal (green) and nasoturbinal (yellow) bones. Maxillary turbinals, which carry respiratory epithelium are shown in blue. The Arctic fox is not among the sample species but its model is used here because of its particular clarity.

**Supplementary figure S2. Time-calibrated phylogeny of sample species**. Tree compiled from published molecular phylogenies [32, 33] (See Main References).

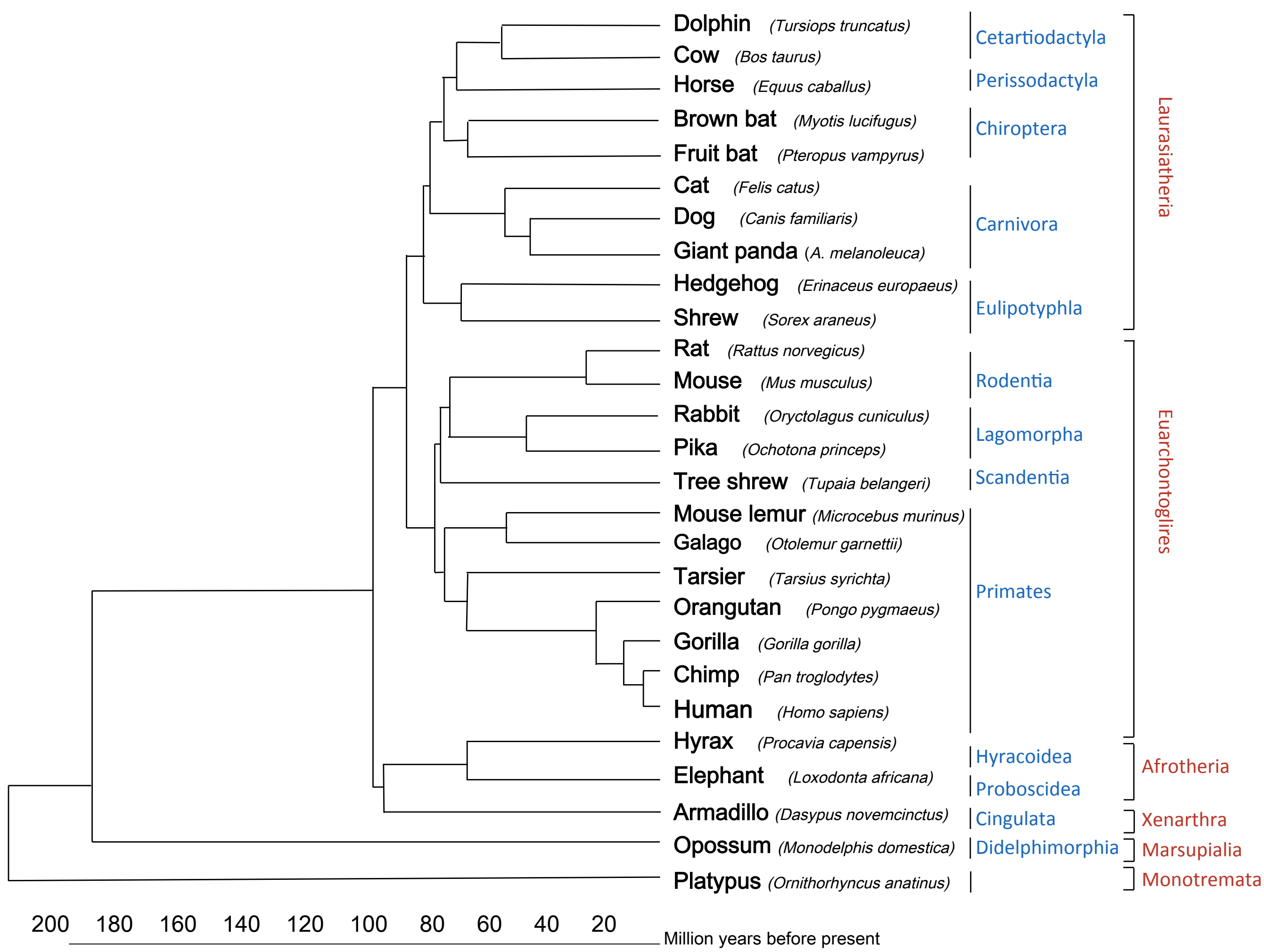

**Supplementary table S3: Key resource table for sample specimens, CT scanning machines and facilities, and digital imaging software.**

| Resource | Source | Identifier |
|---|---|---|
| **Skulls** | | |
| *Ailuropoda melanoleuca* | Institute of Zoology Chinese Academy of Sciences | IZCAS6072 |
| *Bos taurus* | Museum of Vertebrate Zoology | MVZ114370 |
| *Bos taurus* | UCLA Dept. Ecology and Evolutionary Biology | UCLAEEB110_1 |
| *Canis familiaris* | Natural History Museum Los Angeles County | LACM031106 |
| *Canis familiaris* | Natural History Museum Los Angeles County | LACM022825 |
| *Canis familiaris* | Natural History Museum Los Angeles County | LACM30539 |
| *Canis familiaris* | Donald R. Dickey Collection UCLA | UCLA3054 |
| *Canis lupus* | National Museum of Natural History | USNM291011 |
| *Canis lupus* | National Museum of Natural History | USNM507338 |
| *Dasypus novemcinctus* | Natural History Museum Los Angeles County | LACM46145 |
| *Dasypus novemcinctus* | Donald R. Dickey Collection UCLA | UCLA1697 |
| *Equus caballus* | Museum of Vertebrate Zoology | MVZ223018 |
| *Equus caballus* | UCLA Dept. Ecology and Evolutionary Biology | UCLAEEB110_2 |
| *Erinaceus europeus* | Natural History Museum Los Angeles County | LACM58376 |
| *Erinaceus europeus* | Natural History Museum Los Angeles County | LACM58375 |
| *Erinaceus europeus* | Museum of Vertebrate Zoology | MVZ183386 |
| *Felis catus* | UCLA Dept. Ecology and Evolutionary Biology | UCLAEEB110_3 |
| *Felis catus* | UCLA Dept. Ecology and Evolutionary Biology | UCLAEEB110_4 |
| *Gorilla gorilla* | Museum of Vertebrate Zoology | MVZ174521 |
| *Gorilla gorilla* | Donald R. Dickey Collection UCLA | UCLA1788 |
| *Gorilla gorilla* | Donald R. Dickey Collection UCLA | UCLA2367 |
| *Homo sapiens* | Museum of Vertebrate Zoology | MVZ106555 |
| *Homo sapiens* | University of Texas Austin | UTO_HS01 |
| *Homo sapiens* | UCLA Dept. Ecology and Evolutionary Biology | UCLAEEB110_5 |
| *Loxodonta africana* | Natural History Museum Los Angeles County | LACM52471 |
| *Microcebus murinus* | Museum of Vertebrate Zoology | MVZ132535 |
| *Microcebus murinus* | Duke Lemur Center | DLC7006 |
| *Microcebus murinus* | Duke University Primate Center | DUPC098 |
| *Monodelphis domestica* | Museum of Vertebrate Zoology | MVZ144306 |
| *Monodelphis domestica* | Museum of Vertebrate Zoology | MVZ144307 |
| *Mus musculus* | Texas Memorial Museum | TMM3196 |
| *Myotis lucifugus* | American Museum of Natural History | AMNH232239 |
| *Myotis lucifugus* | American Museum of Natural History | AMNH232244 |
| *Ochotona princeps* | Donald R. Dickey Collection UCLA | UCLA17230 |
| *Ochotona princeps* | Museum of Vertebrate Zoology | MVZ42613 |
| *Ornithorynchus anatinus* | Museum of Vertebrate Zoology | MVZ126977 |
| *Ornithorynchus anatinus* | Museum of Vertebrate Zoology | MVZ126978 |
| *Orychtolagus cuniculus* | Natural History Museum Los Angeles County | LACM7601 |
| *Orychtolagus cuniculus* | Natural History Museum Los Angeles County | LACM7603 |

| | | |
|---|---|---|
| *Otolemur garnettii* | Cleveland Museum of Natural History | CMNH_B0748 |
| *Pan troglodytes* | National Museum of Natural History | USNM395820 |
| *Pongo pygmaeus* | Museum of Vertebrate Zoology | MVZ65532 |
| *Pongo pygmaeus* | University of Texas Austin | UTO_49859 |
| *Procavia capensis* | Natural History Museum Los Angeles County | LACM90782 |
| *Procavia capensis* | Texas Memorial Museum | TMM4351 |
| *Pteropus vampyrus* | Donald R. Dickey Collection UCLA | LACM91185 |
| *Pteropus vampyrus* | Donald R. Dickey Collection UCLA | LACM91183 |
| *Pteropus vampyrus* | Museum of Vertebrate Zoology | MVZ116834 |
| *Rattus norvegicus* | Donald R. Dickey Collection UCLA | UCLA6994 |
| *Rattus norvegicus* | Donald R. Dickey Collection UCLA | UCLA9452 |
| *Smilodon fatalis* | Rancho La Brea Tar Pits | LACMRLP_R37376 |
| *Sorex araneus* | Museum of Vertebrate Zoology | MVZ179796 |
| *Tarsius syrichta* | Duke Lemur Center | DLC1406_82 |
| *Tupaia belangeri* | Natural History Museum Los Angeles County | LACM008157 |
| *Tupaia belangeri* | Museum of Vertebrate Zoology | MVZ119721 |
| *Tursiops truncatus* | San Diego Society of Natural History | SDSNH 21212 |
| *Tursiops truncatus* | Natural History Museum Los Angeles County | LACM84269 |
| *Tursiops truncatus* | Natural History Museum Los Angeles County | LACM95828 |
| **High resolution CT scanners** | | |
| GE Phoenix V\|tome\|x s | General Electric Applications Technology | https://gemeasurement.com/ |
| GE Phoenix nanotom s | General Electric Applications Technology | https://gemeasurement.com/ |
| GE Phoenix nanotom m | General Electric Applications Technology | https://gemeasurement.com/ |
| North Star Imaging ACTIS | The University of Texas High-Resolution X-ray Computed Tomography Facility | http://www.ctab.geo.utexas.edu |
| Nikon Metrology XT H 225 ST | Molecular Imaging Center, Univ. of Southern California | http://mic.usc.edu/ |
| Xradia microXCT | The University of Texas High-Resolution X-ray Computed Tomography Facility | http://www.ctab.geo.utexas.edu |
| Siemens SOMATOM Definition AS64 | Ronald Reagan Medical Center UCLA | https://usa.healthcare.siemens.com |
| **Imaging software** | | |
| Mimics v. 15.0-18.0 | Materialise; Leuven, Belgium | http://www.materialise.com |
| 3-Matics v. 7.0.1 | Materialise; Leuven, Belgium | http://www.materialise.com |
| Rhinoceros v. 4 | Robert McNeel and Associates | https://www.rhino3d.com/ |

## CONTACT FOR RESOURCE SHARING.

Further information and requests for resources, scanning parameters, CT scan files, and 3D skull models should be directed to and will be fulfilled by the Lead Contact, Deborah Bird (dbirdseed@gmail.com).

**Supplementary table S4**. **Cribriform plate surface area data for individual specimens**. Abbreviations, AMNH: American Museum of Natural History. CMNH: Cleveland Museum of Natural History. DLC: Duke Lemur Center. DUPC: Duke University Primate Center. IZCAS: Institute of Zoology of the Chinese Academy of Sciences. LACM: Natural History Museum of Los Angeles County. LACMRLP: Rancho La Brea Tar Pits. MVZ: Museum of Vertebrate Zoology. SDSNH: San Diego Society of Natural History. UCLA: Dickey Collection at the University of California Los Angeles. UCLAEEB: UCLA Department of Ecology and Evolutionary Biology. USNM: National Museum of Natural History. UTO: University of Texas Austin. TMM: Texas Memorial Museum**.** *The presence of a cribriform plate in the ethmoid bone of the bottlenose dolphin (*Tursiops truncatus*) could not be established in this study.

| **Species** | **Specimen** | **Sex** | **Cribriform plate surface area (mm$^2$)** |
|---|---|---|---|
| *Ailuropoda melanoleuca* | IZCAS6072 | U | 741.58 |
| *Bos taurus* | MVZ114370 | F | 2482.09 |
| *Bos taurus* | UCLAEEB110_1 | U | 2406.12 |
| *Canis familiaris* | LACM031106 | M | 382.21 |
| *Canis familiaris* | LACM022825 | U | 601.60 |
| *Canis familiaris* | LACM30539 | M | 851.57 |
| *Canis familiaris* | UCLA3054 | U | 446.28 |
| *Canis lupus* | USNM291011 | M | 1045.53 |
| *Canis lupus* | USNM507338 | F | 946.09 |
| *Dasypus novemcinctus* | LACM46145 | M | 425.00 |
| *Dasypus novemcinctus* | UCLA1697 | M | 456.73 |
| *Equus caballus* | MVZ223018 | M | 2321.06 |
| *Equus caballus* | UCLAEEB110_2 | U | 2327.43 |
| *Erinaceus europeus* | LACM58376 | M | 93.44 |
| *Erinaceus europeus* | LACM58375 | F | 81.04 |
| *Erinaceus europeus* | MVZ183386 | M | 104.79 |
| *Felis catus* | UCLAEEB110_3 | M | 188.86 |
| *Felis catus* | UCLAEEB110_4 | U | 134.59 |
| *Gorilla gorilla* | MVZ174521 | F | 165.18 |
| *Gorilla gorilla* | UCLA1788 | M | 261.12 |
| *Gorilla gorilla* | UCLA2367 | F | 135.21 |
| *Homo sapiens* | MVZ106555 | F | 208.91 |
| *Homo sapiens* | UTO_HS01 | M | 171.03 |
| *Homo sapiens* | UCLAEEB110_5 | F | 161.65 |
| *Loxodonta africana* | LACM52471 | F | 17922.00 |
| *Microcebus murinus* | MVZ132535 | F | 12.82 |
| *Microcebus murinus* | DLC7006 | M | 11.02 |
| *Microcebus murinus* | DUPC098 | U | 13.18 |

| | | | |
|---|---|---|---|
| *Monodelphis domestica* | MVZ144306 | F | 24.01 |
| *Monodelphis domestica* | MVZ144307 | M | 23.03 |
| *Mus musculus* | TMM3196 | M | 10.21 |
| *Myotis lucifugus* | AMNH232239 | U | 5.83 |
| *Myotis lucifugus* | AMNH232244 | U | 4.83 |
| *Ochotona princeps* | UCLA17230 | M | 19.29 |
| *Ochotona princeps* | MVZ42613 | M | 19.29 |
| *Ornithorynchus anatinus* | MVZ126977 | M | 22.42 |
| *Ornithorynchus anatinus* | MVZ126978 | M | 24.16 |
| *Orychtolagus cuniculus* | LACM7601 | M | 124.79 |
| *Orychtolagus cuniculus* | LACM7603 | M | 109.74 |
| *Otolemur garnettii* | CMNH_B0748 | U | 39.33 |
| *Pan troglodytes* | USNM395820 | U | 125.47 |
| *Pongo pygmaeus* | MVZ65532 | M | 129.65 |
| *Pongo pygmaeus* | UT49859 | M | 149.27 |
| *Procavia capensis* | LACM90782 | M | 77.33 |
| *Procavia capensis* | UCLATMM4351 | M | 68.16 |
| *Pteropus vampyrus* | LACM91185 | U | 44.92 |
| *Pteropus vampyrus* | LACM91183 | U | 47.67 |
| *Pteropus vampyrus* | MVZ116834 | M | 74.87 |
| *Rattus norvegicus* | UCLA6994 | F | 35.61 |
| *Rattus norvegicus* | UCLA9452 | M | 35.86 |
| *Smilodon fatalis* | LACMRLP_R37376 | U | 1012.00 |
| *Sorex araneus* | MVZ179796 | F | 10.57 |
| *Tarsius syrichta* | DLC1406_82 | F | 3.22 |
| *Tupaia belangeri* | LACM008157 | M | 57.93 |
| *Tupaia belangeri* | MVZ119721 | M | 55.30 |
| *Tursiops truncatus* | SDSNH 21212 | U | NA* |
| *Tursiops truncatus* | LACM84269 | M | NA* |
| *Tursiops truncatus* | LACM95828 | U | NA* |

**Supplementary figure S5. Digitally quantifying CP surface area. (*a*),** Three-dimensional CP model from the French bulldog (*Canis familiaris*) is reconstructed from CT scan data in Mimics imaging program. **(*b*)**, CP foramina are digitally filled to create a generalized continuous surface within the perforate region of the bone. **(*c*)**, Surface area is isolated and calculated with imaging software 3-matic.

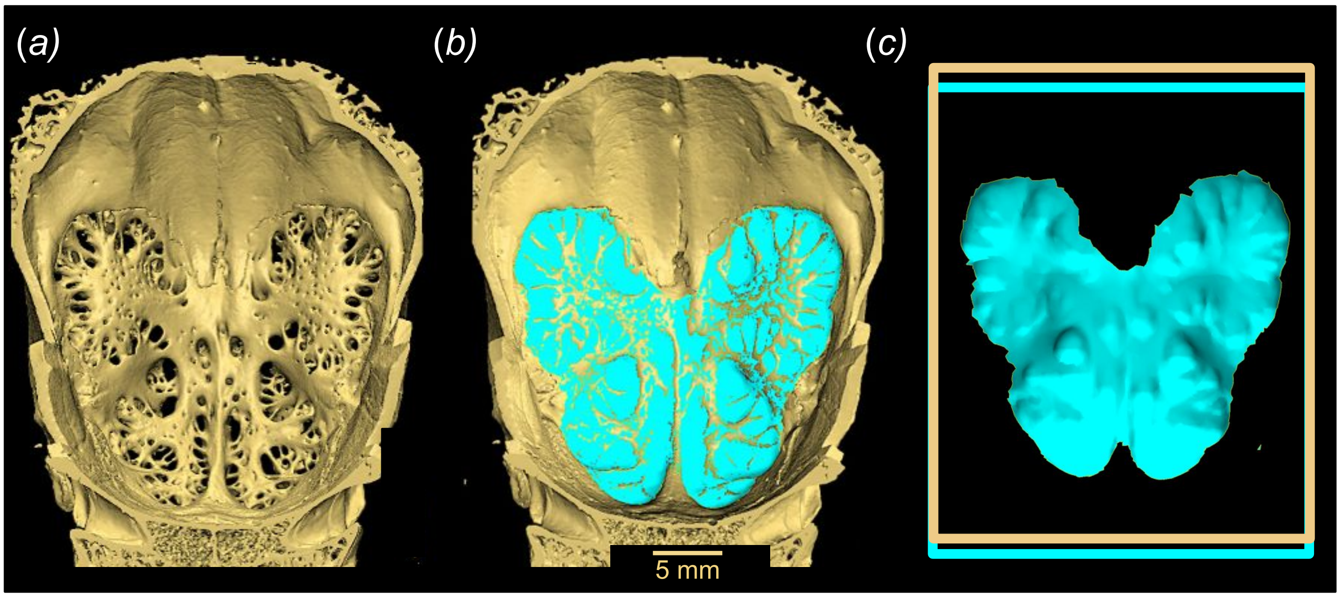

**Supplementary figure S6. Strong linear correlation between cribriform plate (CP) surface area (perforate area) and cumulative cross-sectional area of the CP foramina (log-log) ($r^2$ = 0.91, $P$ < 0.0001, n = 19).** The more exacting metric of total CP foramina area, representing the imprint of olfactory axon bundles in the ethmoid bone, serves to validate CP surface area as a metric of relative olfactory innervation. CP surface area is the preferable metric for future studies, as it is easily quantifiable, even in skulls with some CP damage, such as fossils. CP surface area was measurable here in 26 sample species, while foramina area was measurable in only 19 species. Image on y axis: taken from figure S5. Images on the x axis: left, section of CP bone (red) with splines, (rings of coordinate points) assigned to the perimeters of several foramina in Mimics; right, imaging software Rhinoceros creates non-planar surfaces from the splines then calculates and tallies all foramina areas.

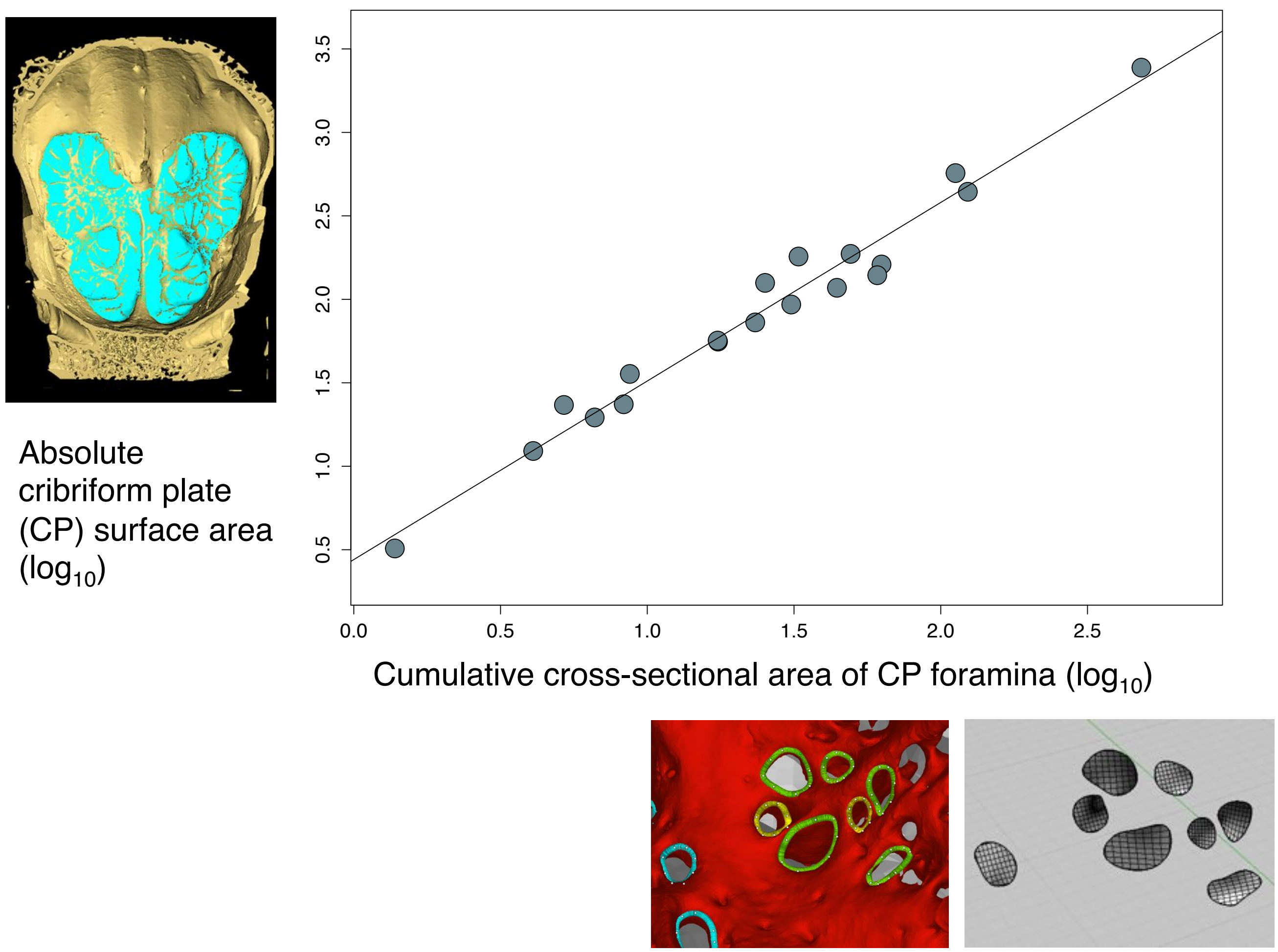

**Supplementary figure S7: 3D skull models showing marked reduction in CP morphology in taxa heavily reliant on non-olfactory sensory modalities.** ***(a)*****,** CP loss viewed in nasal morphology of bottlenose dolphin (*Tursiops truncatus*), which uses echolocation. Pink: Single pair of foramina connecting ethmoid area of the nasal passage to the cranium. Inset, magnification of foramina. ***(b-c)***, Impact of orbit size on CP size constraints, contrasting the tarsier (*Tarsius syrichta*) and armadillo (*Dasypus novemcinctus*). ***(b)***, Tarsier, a visually-specialized nocturnal primate with enlarged, forward facing orbits, has reduced olfactory anatomy. Red: CP squeezed between convergent orbits. ***(c)*****,** By contrast, the armadillo's large CP (red) fills the space between small, laterally oriented, wide set orbits.

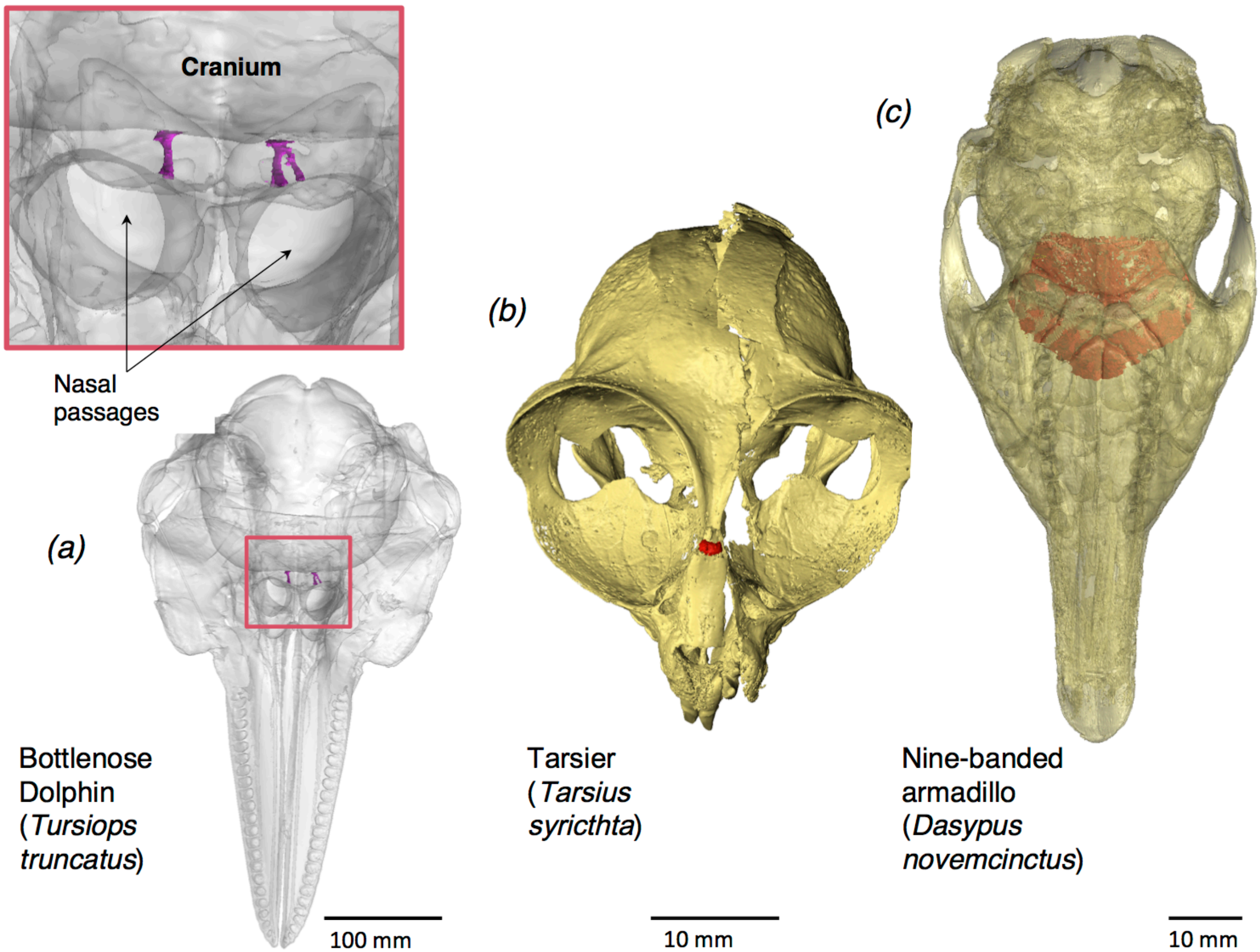

**Supplementary table S8: Morphological and genomic data for sample species.** Abbreviations: CP, cribriform plate; ORG, olfactory receptor gene. Body mass estimates are species means. Where sexual dimorphism was present, we considered the sex of individuals when deriving the species body mass. Individual dog breed body size estimates were averaged to calculate the mean body mass of the dog (*Canis familiaris*). [a]References for body mass and ORG data listed below the table. References for ORG data are found within the reference list in the main text as well. For cribriform plate surface area data of individual specimens, see table S4.

| Species | Common name | n | CP surface area ($mm^2$) | Body mass (kg) | Body mass references[a] | Relative CP surface area | Total ORGs | Functional ORGs | Pseudo-genes | Percent pseudo-genes | ORG data references[a] |
|---|---|---|---|---|---|---|---|---|---|---|---|
| *Ailuropoda melanoleuca* | Giant panda | 1 | 741.58 | 111.600 | 1 | 0.016 | 1235 | 907 | 328 | 0.266 | 22 |
| *Bos taurus* | Cow | 2 | 2444.10 | 453.592 | 2 | 0.214 | 2284 | 1186 | 1057 | 0.463 | 23 |
| *Canis familiaris* | Dog: French bulldog, saluki, borzoi, dachshund | 4 | 570.42 | 21.890 | 3,4,5,4 | 0.274 | 1100 | 811 | 278 | 0.253 | 23 |
| *Canis lupus* | Gray wolf | 2 | 995.81 | 34.875 | 6 | 0.410 | NA | NA | NA | NA | NA |
| *Dasypus novemcinctus* | Nine-banded armadillo | 2 | 440.87 | 5.647 | 7 | 0.472 | 3146 | 1146 | 2000 | 0.636 | 24 |
| *Equus caballus* | Horse | 2 | 2324.24 | 250.000 | 4 | 0.328 | 2658 | 1066 | 1569 | 0.59 | 23 |
| *Erinaceus europaeus* | Hedgehog | 3 | 93.09 | 1.177 | 8 | 0.155 | 625 | 295 | 330 | 0.528 | 24 |
| *Felis catus* | Cat | 2 | 161.72 | 4.750 | 9 | 0.081 | 1052 | 677 | 375 | 0.356 | 25 |
| *Gorilla gorilla* | Gorilla | 3 | 187.17 | 104.167 | 10 | -0.566 | 597 | 263 | 334 | 0.559 | 24 |
| *Homo sapiens* | Human | 3 | 180.53 | 62.000 | 11 | -0.463 | 821 | 396 | 425 | 0.518 | 26 |
| *Loxodonta africana* | African elephant | 1 | 17922.00 | 2766.000 | 12 | 0.650 | 4267 | 1948 | 2230 | 0.523 | 23 |
| *Microcebus murinus* | Mouse lemur | 3 | 12.34 | 0.054 | 13 | -0.018 | 980 | 576 | 404 | 0.412 | 24 |
| *Monodelphis domestica* | Opossum | 2 | 23.52 | 0.071 | 4 | 0.198 | 1492 | 1188 | 294 | 0.197 | 27 |
| *Mus musculus* | Mouse | 1 | 10.21 | 0.015 | 4 | 0.192 | 1366 | 1130 | 236 | 0.173 | 23 |
| *Myotis lucifugus* | Little brown bat | 2 | 5.33 | 0.010 | 4 | 0.015 | 741 | 460 | 281 | 0.379 | 22 |
| *Ochotona princeps* | Pika | 2 | 19.60 | 0.158 | 4 | -0.062 | 803 | 489 | 314 | 0.391 | 24 |
| *Ornithorhynchus anatinus* | Platypus | 2 | 23.29 | 1.484 | 4 | -0.500 | 718 | 265 | 370 | 0.515 | 27 |
| *Oryctolagus cuniculus* | Rabbit | 2 | 117.26 | 1.800 | 14 | 0.158 | 1046 | 768 | 256 | 0.245 | 23 |
| *Otolemur garnettii* | Galago | 1 | 39.33 | 0.760 | 4 | -0.119 | 803 | 433 | 370 | 0.461 | 24 |
| *Pan troglodytes* | Chimpanzee | 1 | 125.47 | 45.000 | 4 | -0.548 | 813 | 380 | 414 | 0.509 | 26 |
| *Pongo pygmaeus* | Orangutan | 2 | 139.46 | 75.000 | 15 | -0.619 | 821 | 296 | 488 | 0.594 | 26 |
| *Procavia capensis* | Rock hyrax | 2 | 72.74 | 4.000 | 16 | -0.231 | 681 | 319 | 362 | 0.532 | 24 |
| *Pteropus vampyrus* | Large fruit bat | 3 | 55.82 | 1.067 | 17 | -0.045 | 670 | 343 | 327 | 0.488 | 24 |
| *Rattus norvegicus* | Rat | 2 | 35.74 | 0.222 | 18 | 0.121 | 1767 | 1207 | 508 | 0.287 | 23 |
| *Smilodon fatalis* | Sabertooth cat | 1 | 1012.00 | 230.000 | 19 | -0.014 | NA | NA | NA | NA | NA |
| *Sorex araneus* | Shrew | 2 | 10.57 | 0.009 | 20 | 0.335 | 1781 | 1031 | 750 | 0.421 | 24 |
| *Tarsius syrichta* | Tarsier | 1 | 3.22 | 0.117 | 21 | -0.778 | 345 | 89 | 256 | 0.742 | 24 |
| *Tupaia belangeri* | Tree shrew | 2 | 56.61 | 0.200 | 4 | 0.344 | 2170 | 979 | 1191 | 0.549 | 24 |
| *Tursiops truncatus* | Bottlenose dolphin | 3 | NA* | 175.000 | 4 | NA | 26 | 12 | 14 | 0.538 | 24 |

**References for supplementary table S8:**


1. Smith, F. A., Lyons, S.K., Ernest, S.K., Jones, K.E. Body mass of late Quaternary mammals. *Ecology* **84,** 3403 (2003).
2. Oklahoma Dept. Agriculture, Food, Forestry, (2015). How much meat? http://www.oda.state.ok.us/
3. French bulldog breed standard (2014). French Bulldog Club of America. http://fbdca.org/

4. Crowley, J., and Adelman, B. (1998). The complete dog book: official publication of the American Kennel Club. New York Howell House.
5. Shiel, R.E., Sist, M., Nachreiner, R.F., Ehrlich, C.P., and Mooney, C.T. (2010). Assessment of criteria used by veterinary practitioners to diagnose hypothyroidism in sighthounds and investigation of serum thyroid hormone concentrations in healthy Salukis. J. Am. Vet. Med. Assoc. *236*, 302–308. (doi:10.2460/javma.236.3.302).
6. Ernest, S.K.M. (2003). Life history characteristics of placental nonvolant mammals. *Ecology* **84**, 3402 (10.1890/02-9002).
7. Wetzel, R.M., and Mondolfi, E. (1979). The subgenera and species of long-nosed armadillos, genus Dasypus L. *Vertebrate ecology in the northern neotropics*, pp.43-47
8. Rautio, A., Valtonen, A., and Kunnasranta, M. (2013). The Effects of Sex and Season on Home Range in European Hedgehogs at the Northern Edge of the Species Range. *Ann. Zool. Fennici* **50**, 107–123. (doi:10.5735/086.050.0110).
9. Myers, P. *et al* (2006). The animal diversity web. *Accessed Oct.* **12,** 2.

10. Jungers, W.L. (1985). Body size and scaling of limb proportions in primates. In Size and scaling in primate biology (Springer), pp. 345–381.
11. Walpole, S.C., Prieto-Merino, D., Edwards, P., Cleland, J., Stevens, G., and Roberts, I. (2012). The weight of nations: an estimation of adult human biomass. *BMC Public Health* **12**, 439. (doi:10.1186/1471-2458-12-439).
12. Laws, R.M. (1970). Elephants and habitats in north Bunyoro, Uganda. *Afr. J. Ecol*. **8**, 163–180. (doi:10.1111/j.1365-2028.1970.tb00838.x).
13. Fietz, J. (1998). Body Mass in Wild Microcebus murinus over the Dry Season. *Folia Primatol*. **69**, 183–190.
14. Nowak, R.M. (1999). Walker's Mammals of the World (JHU Press).
15. Groves, C.P. (1971). Pongo pygmaeus. *Mamm. Species*, 1–6. (doi:10.2307/3503852).
16. Olds, N., and Shoshani, J. (1982). Procavia capensis. Mamm. Species, 1–7. (doi: 10.2307/3503802).
17. McNab, B.K., and Armstrong, M.I. (2001). Sexual dimorphism and scaling of energetics in flying foxes of the genus Pteropus. J. Mammal. *82*, 709–720. (doi:10.1644/1545-1542(2001)082<0709:SDASOE>2.0.CO;2).
18. Glass, G.E., Korch, G.W., and Childs, J.E. (1988). Seasonal and habitat differences in growth rates of wild Rattus norvegicus. J. Mammal. *69*, 587–592. (doi: 10.2307/1381350).
19. Van Valkenburgh, B., Hayward, M.W., Ripple, W.J., Meloro, C., and Roth, V.L. (2015). The impact of large terrestrial carnivores on Pleistocene ecosystems. Proc. Natl. Acad. Sci. *113*, 1–6. (doi:10.1073/pnas.1502554112/-/DCSupplemental).
20. Gębczyński, M. (1965). Seasonal and age changes in the metabolism and activity of Sorex araneus Linnaeus 1758. Acta Theriol. (Warsz). *10*, 303–331.
21. Kappeler, P.M. (1991). Patterns of Sexual Dimorphism in Body Weight among Prosimian Primates. Folia Primatol. *57*, 132–146. (doi:10.1159/000156575).

22. Hughes, G.M., Gang, L., Murphy, W.J., Higgins, D.G., and Teeling, E.C. (2013). Using Illumina next generation sequencing technologies to sequence multigene families in de novo species. Mol. Ecol. Resour. *13*, 510–521. (doi: 10.1111/1755-0998.12087).
23. Niimura, Y., Matsui, A., and Touhara, K. (2014). Extreme expansion of the olfactory receptor gene repertoire in African elephants and evolutionary dynamics of orthologous gene groups in 13 placental mammals. Genome Res. *24*, 1485–1496. (doi:10.1101/gr.169532.113).
24. Hayden, S., Bekaert, M., Crider, T.A., Mariani, S., Murphy, W.J., and Teeling, E.C. (2010). Ecological adaptation determines functional mammalian olfactory subgenomes. Genome Res. *20*, 1–9. (doi:10.1101/gr.099416.109).
25. Montague, M.J., Li, G., Gandolfi, B., Khan, R., Aken, B.L., Searle, S.M.J., Minx, P., Hillier, L.W., Koboldt, D.C., Davis, B.W. (2014). Comparative analysis of the domestic cat genome reveals genetic signatures underlying feline biology and domestication. Proc. Natl. Acad. Sci. U. S. A. *111*, 17230–5. (doi: 10.1101/gr.186668.114)
26. Matsui, A., Go, Y., and Niimura, Y. (2010). Degeneration of olfactory receptor gene repertories in primates: No direct link to full trichromatic vision. Mol. Biol. Evol. *27*, 1192–1200. (doi: 10.1093/molbev/msq003).
27. Niimura, Y., and Nei, M. (2007). Extensive gains and losses of olfactory receptor genes in mammalian evolution. PLoS One *2*, e708. (doi: 10.1371/journal.pone.0000708).

**Supplementary table S9. Assembly statistics for genome assemblies from which olfactory receptor gene counts were extracted.** Abbreviations, BGI: Beijing Genomics Institute; BCM: Baylor College of Medicine; Broad: Broad Institute; ICGSC: International Cat Genome Sequencing Consortium; WU: Washington University. Sources of data: NCBI Assembly, University of California Santa Cruz Genome Browser, Genome Reference Consortium.

| Species | Common name | Assembly name | Coverage x | Contig N50 | Scaffold N50 | Gaps btw scaffolds | Data generation center | Genbank accession number |
|---|---|---|---|---|---|---|---|---|
| *Ailuropoda melanoleuca* | Giant panda | AilMel_1.0 | 60 | 39,886 | 1,281,781 | 0 | BGI | GCA_000004335.1 |
| *Bos taurus* | Cow | Btau_4.0 | 7.1 | 76,397 | 1,949,504 | 2,301 | BCM | GCF_000003205.2 |
| *Canis familiaris* | Dog | canFam2 | 7.6 | 179,651 | 45,337,677 | 86 | Broad | GCA_000002285.1 |
| *Dasypus novemcinctus* | Nine-banded armadillo | Dasnos2.0 | 2.3 | 2,428 | 55,360 | 0 | BCM | GCA_000208655.1 |
| *Equus caballus* | Horse | EquCab2 | 6.8 | 112,381 | 46,749,900 | 51 | Broad | GCA_000002305.1 |
| *Erinaceus europeus* | European hedgehog | eriEur1 | 2 | 2,753 | NA | 0 | Broad | GCA_000181395.1 |
| *Felis catus* | Cat | felCat8 | 14 | 45,189 | 18,072,971 | 303 | ICGSC | GCA_000181335.3 |
| *Gorilla gorilla* | Gorilla | gorGor3.1 | 2.1 | 11,661 | 913,458 | 7,001 | WSI | GCA_000151905.1 |
| *Homo sapiens* | Human | hg18 | 10 | 38,509,590 | 38,509,590 | 301 | multiple | GCF_000001405.12 |
| *Loxodonta africana* | African elephant | Loxafr3.0 | 7 | 69,023 | 46,401,353 | 0 | Broad | GCA_000001905.1 |
| *Microcebus murinus* | Gray mouse lemur | micMur1 | 1.93 | 3,511 | 140,884 | 0 | Broad | GCA_000165445.1 |
| *Monodelphis domestica* | Gray short-tailed opossum | monDom4 | 6.5 | 108,014 | 59,809,810 | 209 | Broad | GCF_000002295.2 |
| *Mus musculus* | Mouse | NCBIm36 | 7 | 24,800 | 16,900,000 | NA | multiple | CAAA01000000 |
| *Myotis lucifugus* | Little brown bat | myoLuc1 | 1.8 | 3,100 | 93,000 | NA | Broad | AAPE01000000 |
| *Ochotona princeps* | American pika | ochPri2 | 1.9 | 3,265 | 88,760 | 0 | Broad | GCA_000164825.1 |
| *Ornithorynchus anatinus* | Platypus | ornAna2 | 6 | 11,544 | 991,605 | 0 | WU | GCA_000002275.2 |
| *Oryctolagus cuniculus* | European rabbit | OryCun2.0 | 7.48 | 64,648 | 35,972,871 | 83 | Broad | GCA_000003625.1 |
| *Otolemur garnettii* | Northern greater galago | otoGar1 | 1.87 | 3,172 | NA | NA | Broad | AAQR01000000 |
| *Pan troglodytes* | Chimpanzee | panTro2 | 6 | 30,554 | 8,803,938 | 3,108 | multiple | GCF_000001515.3 |
| *Pongo pygmaeus* | Bornean orangutan | ponAbe2.0 | 6 | 15,648 | 747,367 | 17,860 | WU | GCA_000001545.3 |
| *Procavia capensis* | Rock hyrax | proCap1 | 2.4 | 3,379 | 24,297 | 0 | BCM | GCA_000152225.1 |
| *Pteropus vampyrus* | Large fruit bat | pteVam1 | 2.9 | 8,527 | 124,060 | 0 | BCM | GCA_000151845.1 |
| *Rattus norvegicus* | Brown rat | rn4 | 7 | 36,847 | 18,621,810 | 270 | BCM | GCF_000001895.3 |
| *Sorex araneus* | Common shrew | sorAra1 | 2 | 3,175 | NA | 0 | Broad | GCA_000181275.1 |
| *Tarsius syrichta* | Phillipine tarsier | tarSyr1 | 2.1 | 2,876 | 12,214 | 0 | WU | GCA_000164805.1 |
| *Tupaia belangeri* | Northern treeshrew | tupBel1 | 2 | 2,974 | NA | 0 | Broad | GCA_000181375.1 |
| *Tursiops truncatus* | Bottlenose dolphin | Turtru1.0 | 2.82 | 9,719 | 166,056 | 0 | BCM | GCA_000151865.1 |

**Supplementary table S10. Summary statistics.** Abbreviations: CP, Cribriform plate; RelCP, Relative cribriform plate size; ORG, Olfactory receptor genes; PGLS, Phylogenetic generalized least squares.

| Regression | n | $r^2$ | *P* value | PGLS $r^2$ | *P* value | Pearson's r | *P* value |
|---|---|---|---|---|---|---|---|
| CP surface area ($\log_{10}$) vs body mass ($\log_{10}$) | 26 | 0.823 | <0.0001 | 0.875 | <0.0001 | 0.91 (.84,.96) | <0.0001 |
| | | | | | | | |
| RelCP vs functional ORG ($\log_{10}$) | 26 | 0.763 | < 0.0001 | 0.7468 | <0.0001 | 0.87 (.73, .95) | <0.0001 |
| RelCP vs functional ORG ($\log_{10}$) (species with ≥ 6x coverage genomes) | 14 | 0.89 | <0.0001 | 0.815 | <0.0001 | 0.94 (.85, .98) | <0.0001 |
| RelCP vs functional ORG ($\log_{10}$) (ORG count in ≤ 2x coverage species adjusted to predicted count for higher-coverage assemblies ) | 26 | 0.841 | <0.0001 | 0.81 | <0.0001 | 0.92 (.81, .97) | <0.0001 |
| | | | | | | | |
| RelCP vs total ORG ($\log_{10}$) | 26 | 0.68 | < 0.0001 | 0.682 | <0.0001 | 0.76 (.63, .86) | <0.0001 |
| RelCP vs total ORG ($\log_{10}$) (ORG count in ≤ 2x coverage species adjusted to pedicted count for higher-coverage assemblies) | 26 | 0.71 | <0.0001 | 0.684 | <0.0001 | 0.77 (.64, .86) | <0.0001 |
| | | | | | | | |
| RelCP vs number of pseudogenes (all species) | 26 | 0.358 | 0.001 | 0.41 | 0.0004 | 0.6 (.3, .77) | 0.0013 |
| RelCP vs number of pseudogenes (6 species with > ~750 pseudogenes) | 6 | 0.74 | 0.027 | 0.723 | 0.032 | 0.86 (.31,.99) | 0.009 |
| RelCP vs number of pseudogenes (20 species with < ~550 pseudogenes) | 20 | 0.09 | 0.19 | 0.009 | 0.68 | -0.31 (-.82,.2) | 0.19 |
| RelCP vs number of pseudogenes (7 species with > ~500 pseudogenes) | 7 | 0.825 | 0.004 | 0.82 | 0.005 | 0.91 (.59,.995) | 0.041 |
| RelCP vs number of pseudogenes (19 species with < ~500 pseudogenes) | 19 | 0.225 | 0.04 | 0.029 | 0.485 | - 0.47 (-.87, .06) | 0.0019 |
| RelCP vs percentage of pseudogenes | 26 | 0.114 | 0.09 | 0.09 | 0.135 | -0.84 (-.95, -.63) | 0.074 |
| | | | | | | | |
| Number functional ORG vs pseudogenes | 26 | 0.465 | 0.0001 | 0.54 | <0.0001 | 0.68 (0.32, .87) | 0.0005 |
| Number functional ORG vs percent pseudogenes | 26 | 0.119 | 0.084 | 0.066 | 0.2 | -0.35 (-.75, .14) | 0.084 |
| | | | | | | | |
| Absolute CP surface area ($\log_{10}$) vs functional ORG ($\log_{10}$) | 26 | 0.22 | 0.015 | 0.27 | 0.006 | 0.47 (-.01, 0.74) | 0.013 |
| Absolute CP surface area ($\log_{10}$) vs functional ORG ($\log_{10}$) elephant omitted | 25 | 0.128 | 0.079 | 0.16 | 0.047 | 0.36 (-.12, 0.66) | 0.078 |

**Supplementary figure S11. Linear regressions in partitioned and non-partitioned data: RelCP vs absolute number of OR pseudogenes.** Among the six species with the largest pseudogene counts, the correlation is $r^2 = 0.744$, $P = 0.026$, PGLS-$r^2 = 0.723$, $P = 0.032$ (red dashed line). There is no significant correlation among the 20 species with the lowest pseudogene counts. A significant linear correlation exists across the entire data, $r^2 = 0.36$, $P = 0.001$, PGLS-$r^2 = 0.41$, $P = 0.004$ (gray dotted line).

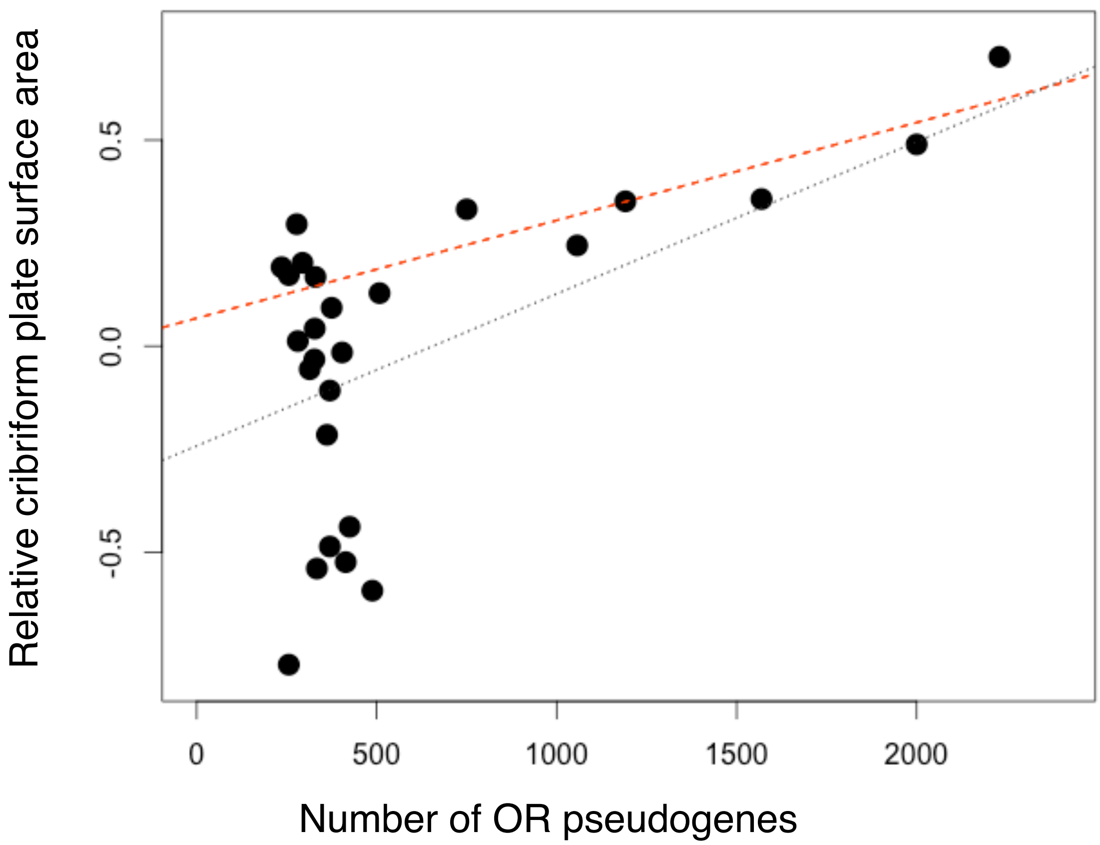

**Supplementary figure S12. Estimating relative CP size (RelCP) to predict the likely position of two non-genome species, the sabertooth cat (*Smilodon fatalis*) and the gray wolf (*Canis lupus*), on our olfactory scale.** ***(a)*****,** Log-log plot of absolute CP surface area regressed against body mass for all sample species plus the extinct felid (*Smilodon fatalis*). Residual value for *Smilodon* was used to estimate RelCP for the sabertooth cat. ***(b)*****,** *Smilodon* CP surface area is smaller for its body size than most of the ten living felid species for which CP data is known. ***(c)*****,** In a regression of CP surface area vs. body size among the sample species plus the gray wolf (*Canis lupus*), the wolf has a larger RelCP than the domestic dog (species mean of four dog breeds), predicting a larger ORG repertoire. ***(d)*** The identical regression plot in main figure 2*d,* here with species labels added.

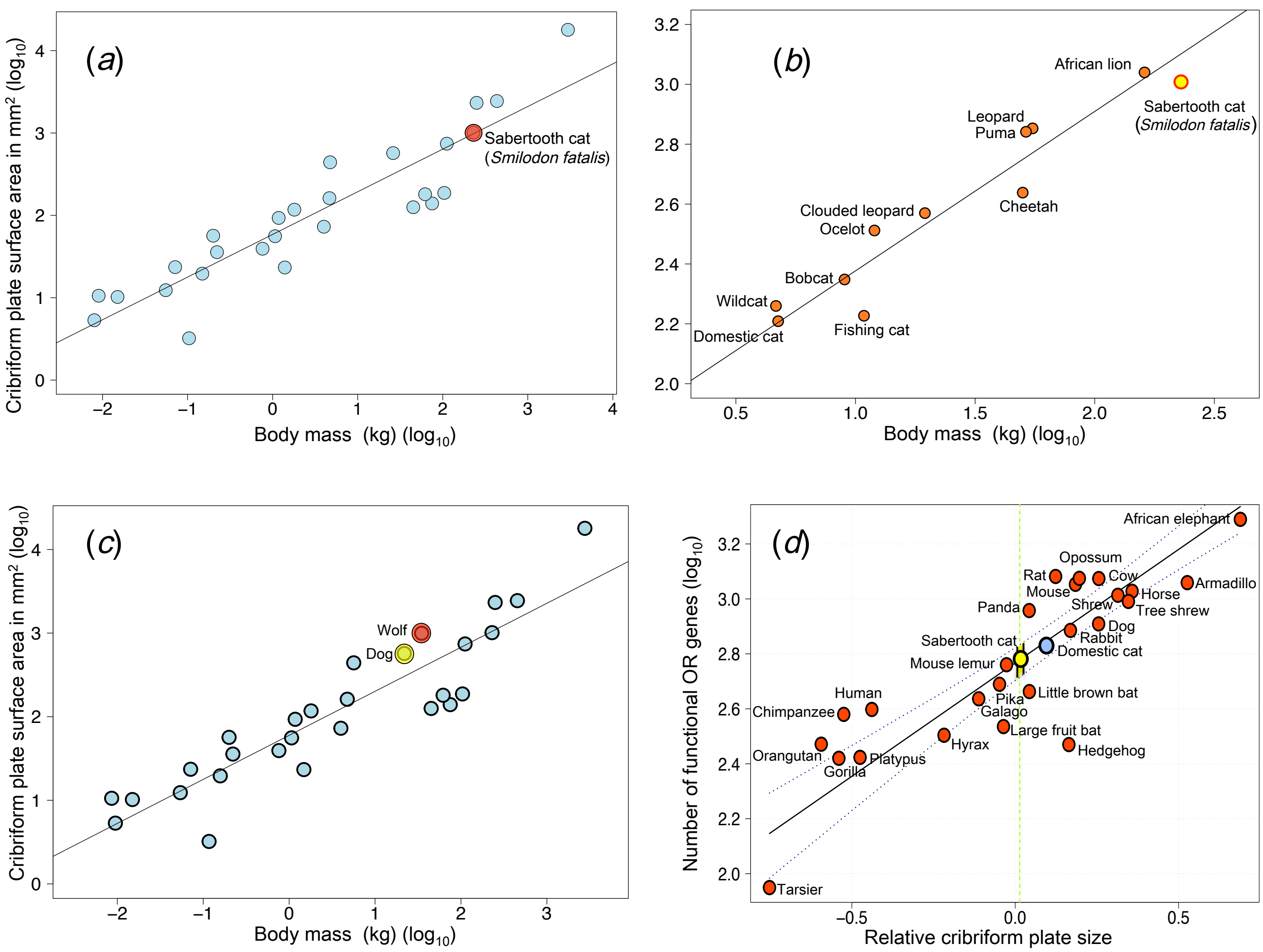

**Supplementary table S13. Sources and morphological data for felid species.** Museums and collections are as follows: FMNH: Field Museum of Natural History; LACM: Museum of Natural History of Los Angeles County; LACMRLP: Rancho La Brea Tar Pits; MMNH: James Ford Bell Museum University of Minnesota, Minneapolis; UCLAEEB: University of California Los Angeles Department of Ecology and Evolutionary Biology. [a]Estimated body masses (in kg) are from [1] except for two species, *Felis catus* [9] and *Smilodon fatalis* [19] (see table S8 references).

| Species | Sex | Specimen | Body Mass[a] | Cribriform plate surface area ($mm^2$) |
|---|---|---|---|---|
| *Acinonyx jubatus* | M | FMNH29635 | 50 | 473.07 |
| *Acinonyx jubatus* | F | FMNH127834 | 50 | 396.43 |
| *Felis catus* | M | UCLAEEB110_4 | 4.65 | 188.86 |
| *Felis catus* | U | UCLAEEB110_3 | 4.65 | 134.59 |
| *Felis silvestris* | M | LACM14480 | 4.65 | 206.27 |
| *Felis silvestris* | F | LACM14474 | 4.65 | 157.46 |
| *Leopardus pardalis* | M | FMNH34339 | 12 | 296.37 |
| *Leopardus pardalis* | F | LACM26789 | 12 | 353.50 |
| *Lynx rufus* | M | UCLA10115 | 9 | 225.13 |
| *Lynx rufus* | F | LACM15254 | 9 | 220.71 |
| *Neofelis nebulosa* | M | LACM31155 | 19.5 | 371.34 |
| *Neofelis nebulosa* | M | USNM282124 | 19.5 | 429.04 |
| *Panthera leo* | M | MMNH17537 | 161.5 | 1149.92 |
| *Panthera leo* | F | MMNH17533 | 161.5 | 1041.53 |
| *Panthera pardus* | M | LACM11704 | 55 | 712.55 |
| *Prionailurus viverrinus* | U | LACM90838 | 10.85 | 184.97 |
| *Prionailurus viverrinus* | F | LACM56718 | 10.85 | 152.30 |
| *Puma concolor* | M | LACM87430 | 51.6 | 701.50 |
| *Puma concolor* | F | LACM85440 | 51.6 | 686.83 |
| *Smilodon fatalis* | U | LACMRLP R37376 | 230 | 820.05 |

**Supplementary figure S14. Adjusting ORG counts for low coverage genomes, or omitting low coverage species, improves correlation between RelCP and functional ORG number.** ***(a)*,** Plot from figure 2*b*; RelCP vs. functional ORGs ($\log_{10}$). Blue circles: species with low coverage (≤ 6x) genome assemblies ($r^2 = 0.76$, $P < 0.0001$). ***(b)*,** Adjusted regression plot. Number of functional ORGs in low-coverage genomes is increased by 39.7%. Percent increase is derived by comparing the number of ORGs extracted from earlier, low-coverage draft genomes to the number from current ≥ 6x coverage assemblies, averaged over four available relevant cases (elephant, dog, cat, rabbit). Adjusted correlation: $r^2 = 0.84$, $P < 0.0001$. Any increase in ORG count in low-coverage species strengthens the correlation, as all but two have relatively few ORGs for their RelCP. ***(c)*,** Omitting species with ≤ 6x genomes strengthens the correlation between RelCP and functional ORGs further ($r^2 = 0.89$, $P < 0.0001$).

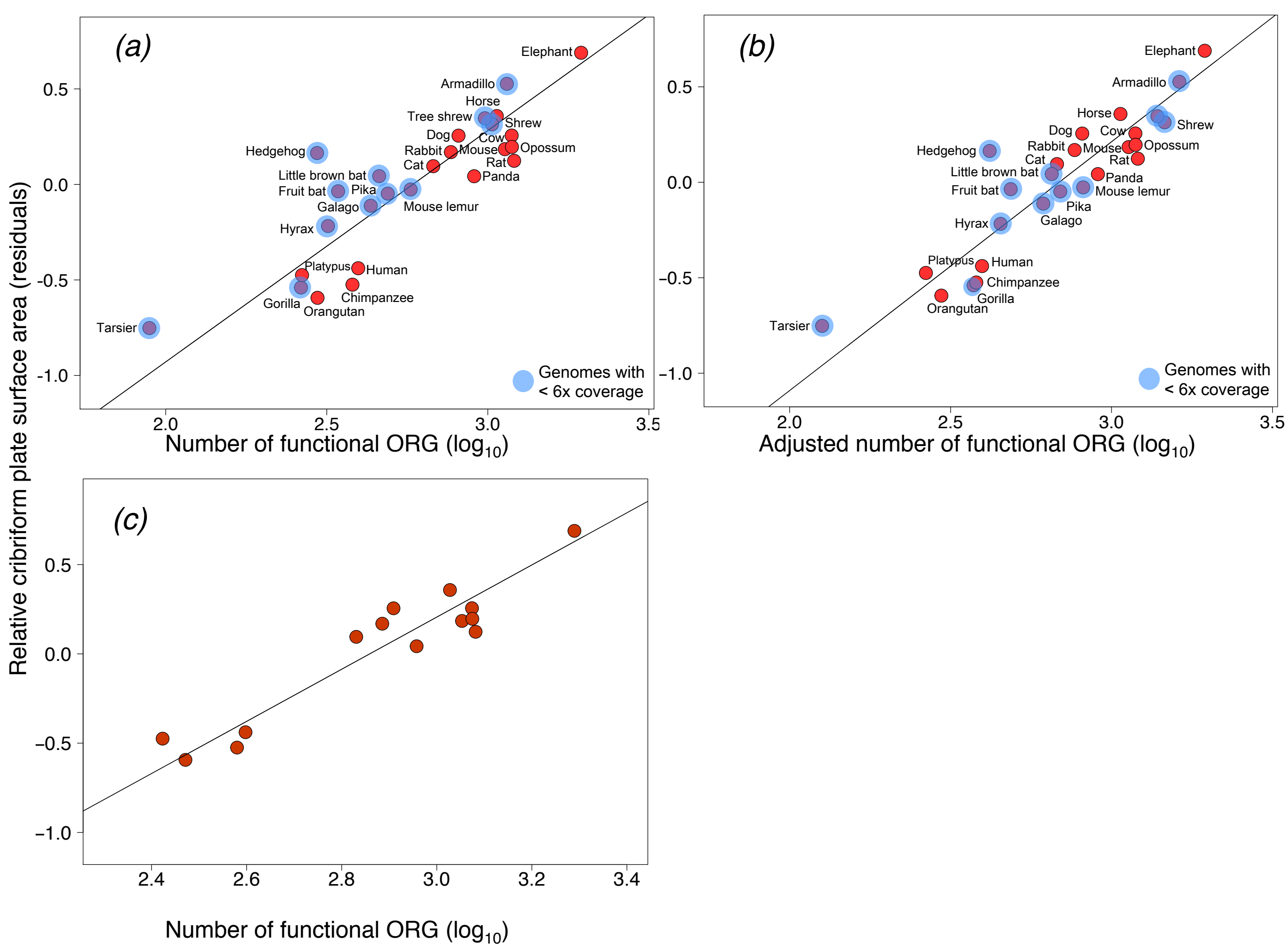

**Supplementary figure S15. High number of OR pseudogenes in species with large RelCP and large ORG repertoires.** ***(a)*,** Inversion of the axes from figure 3*a* showing that species with largest RelCP tend to have highest numbers of OR pseudogenes. ***(b)*,** A similar non-linear, dual pattern emerges when the dependent variable in figure 3*a* is changed from RelCP to number of functional ORG. Species with > ~500 pseudogenes tend to have larger functional ORG repertoires.

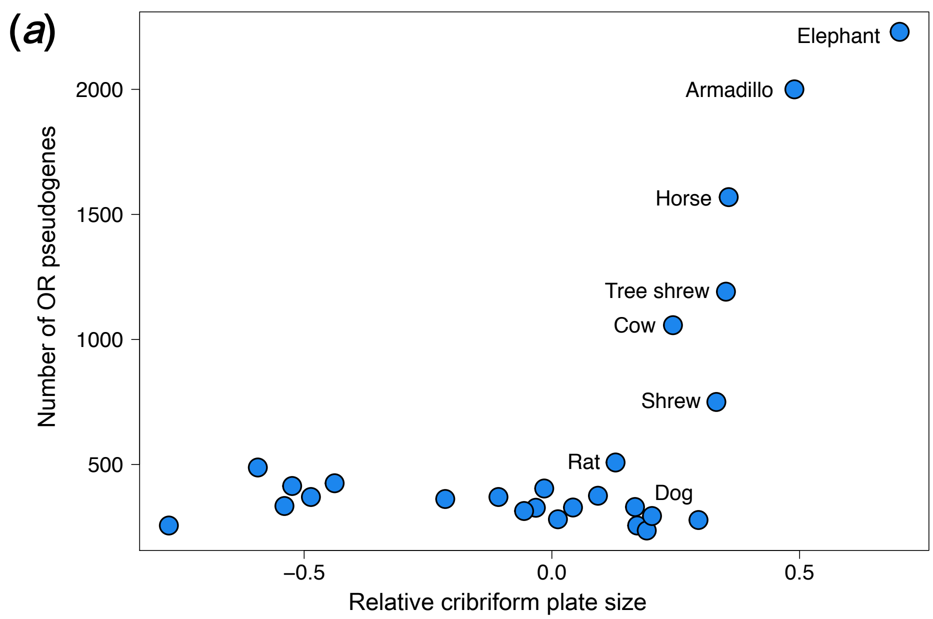


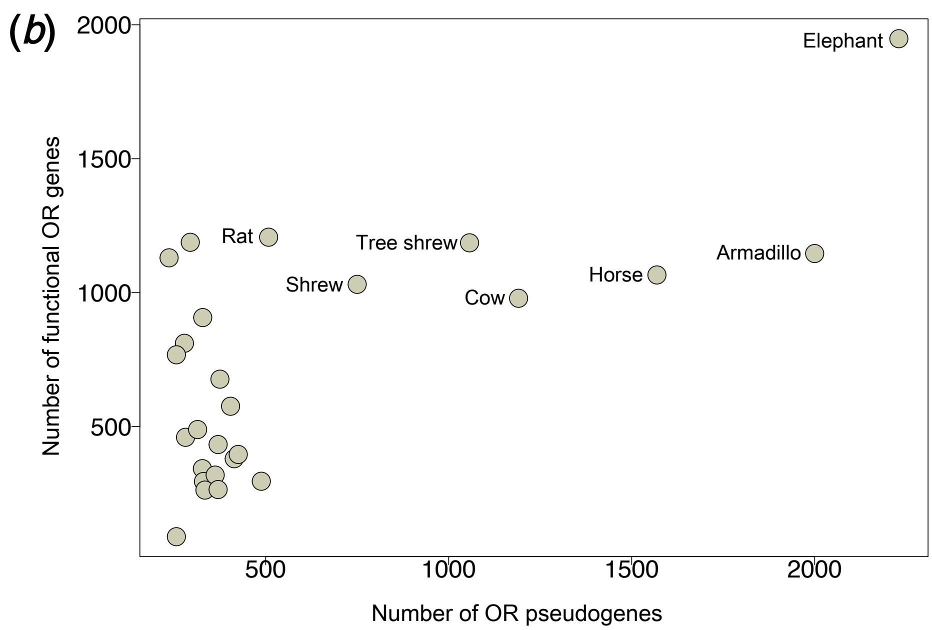

**Supplementary figure S16. Skull pneumatization as possible correlate of large CP size; contrast between elephant and gorilla skulls shown in CT scan images and 3D skull models.** ***(a)*****,** Coronal cross-section slice from CT scan of elephant (*Loxodonta africana*) skull showing ~250 mm pneumatized bone surrounding brain. Scale bar: 100 mm. ***(b)*****,** Dorsal view of elephant skull model. Yellow line: locale of image in *(a)*. Scale bar: 100 mm. ***(c)*****,** Coronal cross-section from CT scan of gorilla (*Gorilla gorilla*) skull; brain surrounded by non-pneumatized cortical bone. Scale bar: 40 mm. ***(d)*****,** Dorsal view of gorilla skull model. Yellow line: locale of image in *(c)*. Red: CP.

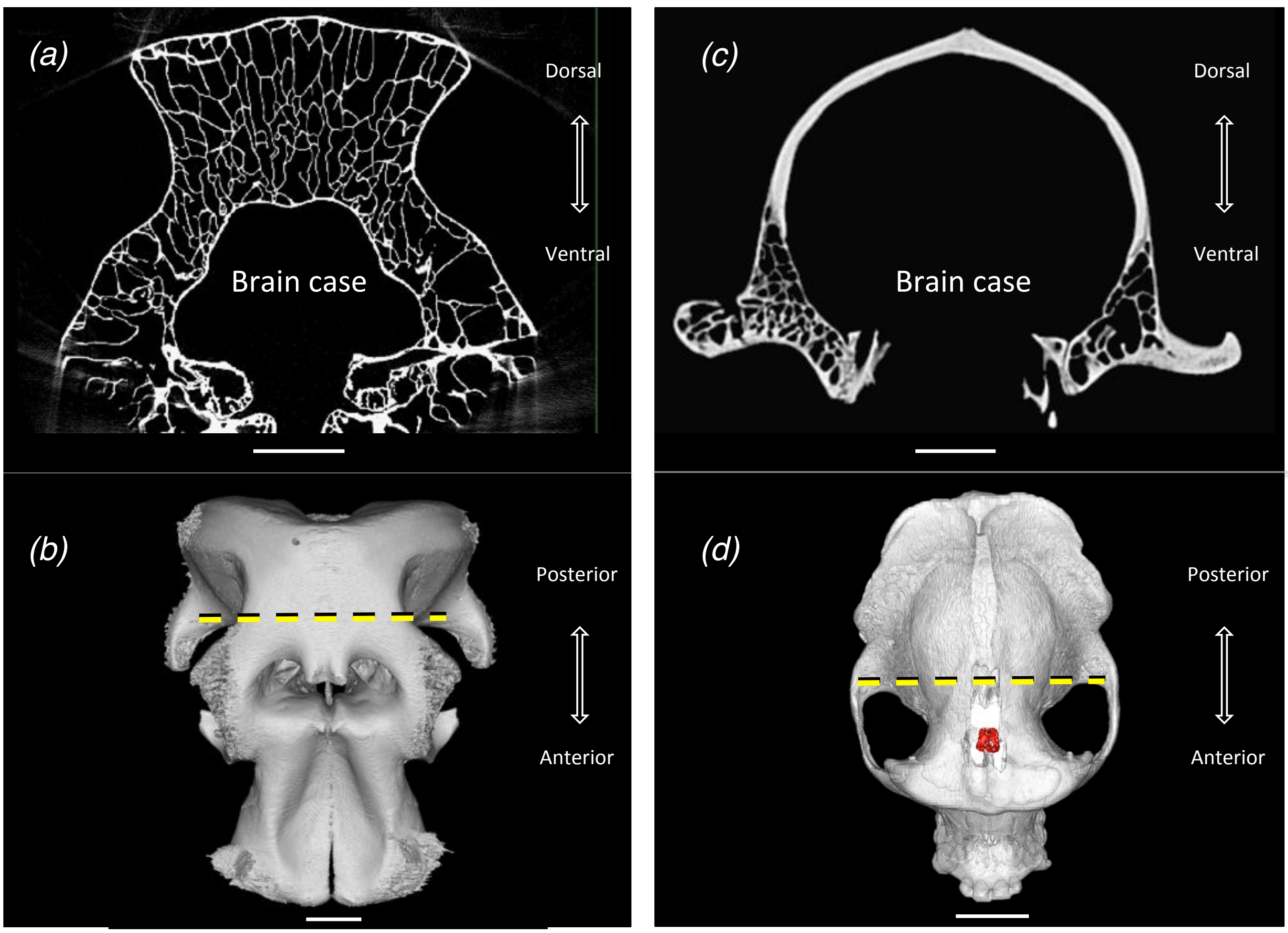

**Supplementary figure S17. Ethmoturbinal complexity matches large RelCP in African elephant; contrast between turbinal-rich elephant skull and turbinal-poor rock hyrax skull shown in CT scan images and 3D skull models.** Ethmoturbinal bones, which carry the olfactory epithelium, are unusually expansive in the African elephant (*Loxodonta africana*). Quantifying turbinal area is beyond the scope of this paper, but here we visually contrast homologous cross-sections from the nasal chamber at the anterior-most extension of the CP in the elephant and its closest living relative, the rock hyrax (*Procavia capensis*), which has a relatively small CP. ***(a)*****,** Anterolateral view of elephant skull model. ***(b)*****,** Coronal cross-section from CT scan of elephant nasal cavity. ***(c)*****,** Hyrax skull model. ***(d)*****,** Coronal slice from CT scan of hyrax nasal cavity. Orange planes: locales of images (*b*) and (c). Blue: turbinals. Red: CP. Scale bars, (*a*): 100mm, (*b*): 20mm, (*c*): 5mm.